



Research article

The global analysis of the SEIR epidemic model with vaccination and population births

Zuoheng Chen^{1,2}, Youhui Su^{2,*}, Qian Wen² and Feng-Lan Tu³

¹ School of Science, Shenyang University of Technology, Shenyang 110870, China

² School of Mathematics and Statistics, Xuzhou University of Technology, Xuzhou 221018, China

³ The Second Affiliated Hospital of Nanchang University, Nanchang 330006, China

*** Correspondence:** Email: suyh02@163.com.

Abstract: This paper constructs a Susceptible-Exposed-Infectious-Recovered (SEIR) model that takes into account the dynamic changes in the birth population and includes both vaccinated and unvaccinated populations. The basic reproduction number R_0 is derived, and its global stability is analyzed. It is proven that when $R_0 < 1$, the disease-free equilibrium point is globally stable. When $R_0 > 1$, there exist an unstable disease-free equilibrium and a unique endemic equilibrium. Subsequently, we conduct the numerical simulations to validate theoretical results and plot data visualizations for various scenarios. In addition, the parameter sensitivity analysis and the forward bifurcation of the model are performed to examine how each system parameter specifically affects disease transmission. Our results offer practical insights for public health planning, particularly in optimizing vaccination strategies in populations with high birth rates or waning immunity.

Keywords: SEIR model; vaccination; bifurcation; global stability; basic reproduction number

1. Introduction

Infectious diseases profoundly affect humanity and individual health. With the advancement of science and technology, some infectious diseases have been eradicated through modern interventions. However, some infectious diseases have evolved new modes of transmission or form as human society develops, such as avian flu, H1N1 influenza, and COVID-19. Infectious diseases not only threaten individual health, but their large-scale outbreaks may also cause shortages of medical resources, declines in productivity, public panic, and social unrest, all of which have profound negative effects on economic growth and social order. Therefore, the effective prevention and control of infectious diseases have become important challenges in global governance. By strengthening control measures,

public health can be effectively safeguarded, social stability maintained, and economic development promoted [1–6].

The Susceptible-Exposed-Infectious-Recovered (SEIR) model originates from the foundational research of Kermack and McKendrick [7], who were pioneers in introducing the Susceptible-Infectious-Recovered (SIR) model in 1927. Their innovative study focused on analyzing the mechanisms underlying the transmission of infectious diseases. The SEIR model, which builds upon the SIR model [8, 9], was designed to account for a critical feature of infectious diseases: incubation period, which more accurately represents the true progression of numerous infectious diseases, such as Ebola, HIV/AIDS, and COVID-19, where individuals may be infected but not yet capable of transmitting the disease [10, 11]. By introducing the exposed category, the model incorporates an extra parameter that can be determined based on existing data. This improvement enables a more precise calculation of key epidemiological factors, including the transmission rate, incubation duration, and other relevant parameters. Keeling and Rohani [12] proposed the following classical SEIR epidemic disease model:

$$\begin{cases} \frac{dS}{dt} = \Lambda - \beta IS - \delta S, \\ \frac{dE}{dt} = \beta IS - (\sigma + \delta)E, \\ \frac{dI}{dt} = \sigma E - (\theta + \delta)I, \\ \frac{dR}{dt} = \theta I - \delta R. \end{cases} \quad (1.1)$$

Here initial population is divided into four classes: susceptible $S(t)$, exposed $E(t)$, infected $I(t)$, and recovered $R(t)$, with t being the time variable. The parameter Λ represents the rate of emergence of new individuals per time unit, δ stands for the natural death rate per capita, β is the transmission rate of diseases, σ denotes the rate of progression from exposed to infectious, and θ refers to the recovery rate of infected individuals. Based on this model (1.1), Yang et al. [13] considered an infectious disease model with saturated incidence rate, where the incidence rate takes into account the behavioral changes of individuals, and by choosing appropriate parameters, they ensured the contact rate remained bounded. Upadhyay et al. [14] developed an SEIR model that incorporates a Crowley-Martin-type incidence rate along with Holling type II and III treatment rates. The analysis of infection spread dynamics and its control was carried out for both types of treatment functions. Khan et al. [15] investigated an SEIR endemic model with age structure and formulated an abstract Cauchy problem to demonstrate the well-posedness of the model.

Traditional models mainly consider the transition processes between susceptible, exposed, infected, and recovered individuals [16, 17]. However, many existing models overlook two critical biological and demographic factors: dynamic vaccination uptake and population renewal through births. From a biological perspective, vaccination directly reduces the density of susceptible population and alters transmission dynamics, while birth inflows continuously introduce new susceptibles, especially when vaccination coverage at birth is incomplete. These factors are crucial for understanding long-term endemic persistence and the effectiveness of immunization programs.

In this paper, we develop an SEIR model that explicitly incorporates continuous vaccination of susceptibles and demographic renewal via births, with a proportion p of newborns vaccinated at birth. Unlike previous studies that often assume constant population or instantaneous vaccination coverage [18–25], our model captures the continuous flow of individuals into the vaccinated and unvaccinated compartments, reflecting real-world vaccination campaigns and birth processes.

By separating the birth input into vaccinated and unvaccinated streams, which more accurately represent the impact of neonatal vaccination policies on herd immunity. The model includes ongoing vaccination of susceptibles and loss of immunity (δ), which allows us to study the interplay between vaccination efforts and natural immunity decay. We establish global stability of both disease-free and endemic equilibria using Lyapunov and geometric methods, providing theoretical guarantees under biologically relevant parameter ranges. Furthermore, the bifurcation analysis and sensitivity analysis are performed to identify key parameters influencing disease spread and control. Our results offer practical insights for public health planning, particularly in optimizing vaccination strategies in populations with high birth rates or waning immunity.

The structure of this paper is as follows: The model framework is established in Section 2. In Section 3, the existence and uniqueness of both disease-free equilibrium and endemic equilibrium are analyzed, accompanied by the formal derivation of the basic reproduction number. In Section 4, the global stability of the disease-free equilibrium is systematically investigated through Lyapunov methods and geometric approaches. The forward bifurcation analyses are performed in Section 5. In Section 6, a special epidemiological scenario is specifically examined. Comprehensive numerical simulations of the proposed model are conducted in Section 7. Finally, the parameter sensitivity analyses are performed to quantify their impacts on the basic reproduction number in Section 8.

2. Model formulation

Based on the progression of the disease, we divide the population into four categories: susceptible (S), exposed (E), infected (I), and recovered (R). Let $S(t)$, $E(t)$, $I(t)$, and $R(t)$ represent the number of individuals in each category at time t . Therefore, the total population at time t is given by $N(t) = S(t) + E(t) + I(t) + R(t)$.

The parameter β characterizes the transmission rate of the disease, ε represents the rate which asymptomatic individuals become infected, γ represents the rate which infected individuals recover, and σ represents the vaccination rate for susceptible individuals. δ represents the rate which recovered individuals lose immunity and become susceptible. We also consider population dynamics, with birth rate b and death rate μ . Additionally, assume that a proportion p of newborns are vaccinated, and the remaining $(1 - p)$ enter the susceptible class as unvaccinated individuals.

Based on the above assumptions, the SEIR model can be described by the following system of equations:

$$\begin{cases} \frac{dS}{dt} = b(1 - p) - \beta S I - (\mu + \sigma) S + \delta R, \\ \frac{dE}{dt} = \beta S I - (\varepsilon + \mu) E, \\ \frac{dI}{dt} = \varepsilon E - (\gamma + \mu) I, \\ \frac{dR}{dt} = bp + \gamma I - (\delta + \mu) R + \sigma S. \end{cases} \quad (2.1)$$

We assume all the parameters are positive. In Figure 1, we plot the flow dynamics of the system (2.1), and the specific parameter values are shown in Table 1 in Section 7.

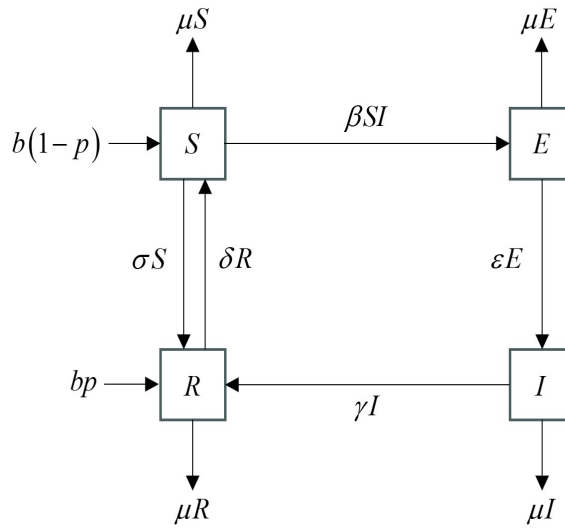


Figure 1. A sketch of the SEIR transmission scheme.

Lemma 2.1. *The feasible region Ω defined by*

$$\Omega = \left\{ (S, E, I, R) \in \mathbb{R}_+^4 : S + E + I + R = \frac{b}{\mu} \right\}$$

is positively invariant for the system (2.1). If the initial condition $(S(0), E(0), I(0), R(0)) \in \Omega$, then the solution $(S(t), E(t), I(t), R(t)) \in \Omega$ for all $t \geq 0$.

Proof. Summing up the equations in system (2.1) yields

$$\frac{dN}{dt} = b - \mu N,$$

where $N(t) = S(t) + E(t) + I(t) + R(t)$. This is a linear differential equation with solution

$$N(t) = N(0)e^{-\mu t} + \frac{b}{\mu}(1 - e^{-\mu t}).$$

If the initial condition satisfies $N(0) = \frac{b}{\mu}$, then

$$N(t) = \frac{b}{\mu}e^{-\mu t} + \frac{b}{\mu}(1 - e^{-\mu t}) = \frac{b}{\mu}.$$

Thus, $N(t) = \frac{b}{\mu}$ for all $t \geq 0$, meaning the solution remains in Ω . Additionally, since all parameters are positive and the system is nonnegative, the solution stays in \mathbb{R}_+^4 . Therefore, Ω is a positively invariant set for the system (2.1).

As the parameters of (2.1) are locally Lipschitz continuous, system (2.1) has a unique local maximal solution $(S(t), E(t), I(t), R(t))$ for all $t \in [0, \tau)$, satisfying the initial conditions, where τ is the explosion time. Below, we shall prove given non-negative initial conditions; the variables remain non-negative and globally defined ($\tau = \infty$) for all $t \in [0, \tau)$.

Theorem 2.2. If $S(0) \geq 0, E(0) \geq 0, I(0) \geq 0, R(0) \geq 0$, then $S(t) > 0, E(t) > 0, I(t) > 0, R(t) > 0$, for all $t \geq 0$, that is, the system (2.1) is globally nonnegative.

Proof. Assume there exists a time point $t > 0$, at which at least one variable becomes negative for the first time. Due to the non-negative initial conditions and the continuity of the solution, we define:

$$t_0 = \inf \{t > 0 : \min\{S(t), E(t), I(t), R(t)\} < 0\}.$$

By continuity, $t_0 > 0$, and for all $t \in [0, t_0]$, we have $S(t) \geq 0, E(t) \geq 0, I(t) \geq 0, R(t) \geq 0$. However, at t_0 , at least one variable becomes zero with a non-positive derivative. We consider each variable's potential to become negative for the first time individually and derive a contradiction.

$S(t)$ becomes negative for the first time. Assume that at t_0 , $S(t_0) = 0$, and $\frac{dS}{dt} \Big|_{t=t_0} \leq 0$. From the equation in system (2.1):

$$\frac{dS}{dt} = b(1-p) - \beta S I - (\mu + \sigma)S + \delta R,$$

at $t = t_0$, $S(t_0) = 0$, thus

$$\frac{dS}{dt} \Big|_{t=t_0} = b(1-p) + \delta R(t_0),$$

since $b(1-p) > 0$ and $R(t_0) \geq 0$. Because t_0 is the time when a variable becomes negative for the first time, and $R(t)$ is non-negative on $[0, t_0]$, we have $\frac{dS}{dt} \Big|_{t=t_0} \geq b(1-p) > 0$, which contradicts $\frac{dS}{dt} \Big|_{t=t_0} \leq 0$. Therefore, $S(t)$ cannot become negative for the first time.

$E(t)$ becomes negative for the first time. Assume that at t_0 , $E(t_0) = 0$, and $\frac{dE}{dt} \Big|_{t=t_0} \leq 0$. From the equation in system (2.1):

$$\frac{dE}{dt} = \beta S I - (\varepsilon + \mu)E,$$

at $t = t_0$, $E(t_0) = 0$, thus

$$\frac{dE}{dt} \Big|_{t=t_0} = \beta S(t_0)I(t_0),$$

since $S(t_0) \geq 0$ and $I(t_0) \geq 0$, we have $\frac{dE}{dt} \Big|_{t=t_0} \geq 0$. Combining this with $\frac{dE}{dt} \Big|_{t=t_0} \leq 0$, we get $\frac{dE}{dt} \Big|_{t=t_0} = 0$, i.e., $\beta S(t_0)I(t_0) = 0$. This implies that $E(t)$ remains zero at t_0 but does not become negative. Therefore, $E(t)$ cannot become negative for the first time.

$I(t)$ becomes negative for the first time. Assume that at t_0 , $I(t_0) = 0$, and $\frac{dI}{dt} \Big|_{t=t_0} \leq 0$. From the equation in system (2.1):

$$\frac{dI}{dt} = \varepsilon E - (\gamma + \mu)I$$

at $t = t_0$, $I(t_0) = 0$, thus

$$\frac{dI}{dt} \Big|_{t=t_0} = \varepsilon E(t_0),$$

since $E(t_0) \geq 0$, we have $\frac{dI}{dt} \Big|_{t=t_0} \geq 0$. Combining this with $\frac{dI}{dt} \Big|_{t=t_0} \leq 0$, we get $\frac{dI}{dt} \Big|_{t=t_0} = 0$, i.e., $\varepsilon E(t_0) = 0$. This implies that $I(t)$ remains zero at t_0 but does not become negative. Therefore, $I(t)$ cannot become negative for the first time.

$R(t)$ becomes negative for the first time. Assume that at t_0 , $R(t_0) = 0$, and $\frac{dR}{dt} \Big|_{t=t_0} \leq 0$. From the equation in system (2.1):

$$\frac{dR}{dt} = bp + \gamma I - (\delta + \mu)R + \sigma S,$$

at $t = t_0$, $R(t_0) = 0$, thus

$$\frac{dR}{dt} \Big|_{t=t_0} = bp + \gamma I(t_0) + \sigma S(t_0),$$

since $bp > 0$, $\gamma I(t_0) \geq 0$, and $\sigma S(t_0) \geq 0$, we have $\frac{dR}{dt} \Big|_{t=t_0} \geq bp > 0$, which contradicts $\frac{dR}{dt} \Big|_{t=t_0} \leq 0$. Therefore, $R(t)$ cannot become negative for the first time.

Since all cases lead to contradictions, the assumption fails. Therefore, for all $t \geq 0$, we have $S(t) > 0$, $E(t) > 0$, $I(t) > 0$, $R(t) > 0$.

3. The basic reproduction number

In this section, we present the disease-free equilibrium point and the basic reproduction ratio R_0 for the systems (2.1).

To obtain the disease-free equilibrium, we set the four equations in the system (2.1) to zero, and assume $E = 0$ and $I = 0$. Accordingly, we obtain the following equations:

$$bp - (\delta + \mu)R_0 + \sigma S_0 = 0,$$

and

$$b(1 - p) - (\mu + \sigma)S_0 + \delta R_0 = 0.$$

We solve the disease-free equilibrium point $P_0 = (S_0, E_0, I_0, R_0)$ of the above equation

$$P_0 = (S_0, E_0, I_0, R_0) = \left(\frac{b(\delta + \mu - \mu p)}{\mu(\mu + \delta + \sigma)}, 0, 0, \frac{b(\sigma + \mu p)}{\mu(\mu + \delta + \sigma)} \right). \quad (3.1)$$

We use the next-generation matrix algorithm (see [26]) to define the basic reproduction number of the system (2.1) as follows:

$$R_0 = \rho(FV^{-1}).$$

Let $x = (S, E, I, R)^T$, then the system (2.1) can be written in the following form:

$$\dot{x} = \mathcal{F}(x) - \mathcal{V}(x),$$

where

$$\mathcal{F}(x) = \begin{bmatrix} 0 \\ \beta S I \\ 0 \\ 0 \end{bmatrix}, \quad \mathcal{V}(x) = \begin{bmatrix} -b(1 - p) + \beta S I + (\mu + \sigma)S - \delta R \\ (\varepsilon + \mu)E \\ -\varepsilon E + (\gamma + \mu)I \\ -bp - \gamma I + (\delta + \mu)R - \sigma S \end{bmatrix}.$$

The Jacobian matrices of $\mathcal{F}(x)$ and $\mathcal{V}(x)$ at the disease-free equilibrium E_0 are as follows:

$$J[\mathcal{F}(P_0)] = \begin{bmatrix} 0 & 0 & 0 & 0 \\ \beta I_0 & 0 & \beta S_0 & 0 \\ 0 & 0 & 0 & 0 \\ 0 & 0 & 0 & 0 \end{bmatrix},$$

and

$$J[\mathcal{V}(P_0)] = \begin{bmatrix} \beta I_0 + (\mu + \sigma) & 0 & \beta S_0 & -\delta \\ 0 & \varepsilon + \mu & 0 & 0 \\ 0 & -\varepsilon & \gamma + \mu & 0 \\ -\sigma & 0 & -\gamma & \delta + \mu \end{bmatrix}.$$

Using the next-generation matrix algorithm [26], we can calculate the basic reproduction number by utilizing two equations corresponding to the infection categories, namely the exposed class (E) and the infectious class (I). This is represented by the matrices F and V below:

$$F = \begin{bmatrix} \beta I_0 & \beta S_0 \\ 0 & 0 \end{bmatrix}, V = \begin{bmatrix} \varepsilon + \mu & 0 \\ -\varepsilon & \gamma + \mu \end{bmatrix},$$

$$V^{-1} = \frac{1}{(\varepsilon + \mu)(\gamma + \mu)} \begin{bmatrix} \gamma + \mu & 0 \\ \varepsilon & \varepsilon + \mu \end{bmatrix}, \quad FV^{-1} = \begin{bmatrix} \frac{\beta S_0 \varepsilon}{(\varepsilon + \mu)(\gamma + \mu)} & \frac{\beta S_0}{\gamma + \mu} \\ 0 & 0 \end{bmatrix},$$

and

$$\rho(FV^{-1}) = \begin{vmatrix} \lambda - \frac{\beta S_0 \varepsilon}{(\varepsilon + \mu)(\gamma + \mu)} & -\frac{\beta S_0}{\gamma + \mu} \\ 0 & \lambda \end{vmatrix} = \lambda \left[\lambda - \frac{\beta S_0 \varepsilon}{(\varepsilon + \mu)(\gamma + \mu)} \right],$$

where $\lambda_1 = 0$, $\lambda_2 = \frac{\beta S_0 \varepsilon}{(\varepsilon + \mu)(\gamma + \mu)}$. The basic reproduction number is given by $R_0 = \rho(FV^{-1})$, that is

$$R_0 = \frac{\beta \varepsilon}{(\varepsilon + \mu)(\gamma + \mu)} \cdot \frac{b(\delta + \mu - \mu p)}{\mu(\mu + \delta + \sigma)}. \quad (3.2)$$

In fact, if $R_0 > 1$, there exists a unique endemic equilibrium point. Setting the equations in the system (2.1) to 0, we obtain the following equations:

$$\begin{cases} b(1 - p) - \beta S^* I^* - (\mu + \sigma) S^* + \delta R^* = 0, \\ \beta S^* I^* - (\varepsilon + \mu) E^* = 0, \\ \varepsilon E^* - (\gamma + \mu) I^* = 0, \\ b p + \gamma I^* - (\delta + \mu) R^* + \sigma S^* = 0. \end{cases}$$

Solving these equations, we obtain the unique endemic equilibrium point $P^* = (S^*, E^*, I^*, R^*)$, where

$$S^* = \frac{(\varepsilon + \mu)(\gamma + \mu)}{\beta \varepsilon},$$

$$E^* = \frac{\gamma + \mu}{\varepsilon} I^*,$$

$$I^* = \frac{\mu(\mu + \delta + \sigma)(R_0 - 1)(\varepsilon + \mu)(\gamma + \mu) + \sigma(\beta - \delta)(\varepsilon + \mu)(\gamma + \mu)}{\beta \mu [\delta(\varepsilon + \gamma + \mu) + \varepsilon \gamma + \mu(\varepsilon + \gamma + \mu)]},$$

and

$$R^* = \frac{\beta \varepsilon (b p + \gamma I^*) + \sigma (\varepsilon + \mu)(\gamma + \mu)}{\beta \varepsilon (\delta + \mu)}.$$

4. Global stability analysis

In this section, we show that the disease-free equilibrium point P_0 and the endemic equilibrium P^* are globally asymptotically stable under some conditions.

From (3.1), the disease-free equilibrium point is given by

$$P_0 = (S_0, E_0, I_0, R_0) = \left(\frac{b(\delta + \mu - \mu p)}{\mu(\mu + \delta + \sigma)}, 0, 0, \frac{b(\sigma + \mu p)}{\mu(\mu + \delta + \sigma)} \right).$$

We now establish its global stability property in the following theorem.

Theorem 4.1. *If $R_0 \leq 1$, then the disease-free equilibrium point P_0 is globally asymptotically stable on Ω .*

Proof. Define the Lyapunov function as follows:

$$V = E + kI.$$

Taking the time derivative along the system (2.1), we have

$$\begin{aligned}\dot{V} &= \dot{E} + k\dot{I} \\ &= \beta S I - (\varepsilon + \mu) E + k [\varepsilon E - (\gamma + \mu) I] \\ &= [\beta S - k(\gamma + \mu)] I + [\varepsilon - (\varepsilon + \mu)] E \\ &\leq \left[\frac{\beta b(\delta + \mu - \mu p)}{\mu(\mu + \delta + \sigma)} - k(\gamma + \mu) \right] I + [\varepsilon - (\varepsilon + \mu)] E.\end{aligned}$$

Let $k = \frac{\varepsilon + \mu}{\varepsilon} > 0$, then

$$\begin{aligned}\dot{V} &\leq \left[\frac{\beta b(\delta + \mu - \mu p)}{\mu(\mu + \delta + \sigma)} - \frac{1}{\varepsilon} (\varepsilon + \mu)(\gamma + \mu) \right] I \\ &= \frac{1}{\varepsilon} (\varepsilon + \mu)(\gamma + \mu)(R_0 - 1) I.\end{aligned}$$

In addition, $\dot{V} = 0$ if and only if $E = I = 0$. Substituting $E = I = 0$ into the system (2.1), we obtain $S \rightarrow S_0$ and $R \rightarrow R_0$ as $t \rightarrow \infty$. Substituting $S = S_0$ and $R = R_0$ into the system (2.1), we get $E \rightarrow 0$ and $I \rightarrow 0$ as $t \rightarrow \infty$. Therefore, V is a Lyapunov function on Ω , and the largest invariant set $(S, E, I, R) : V = 0$ is a singleton set P_0 . By the LaSalle invariance principle [27], when $R_0 \leq 1$, all solutions of the system (2.1) will tend to P_0 as $t \rightarrow \infty$.

Definition 4.2. *The system (2.1) is said to be uniformly persistent if there exists a constant $0 < \epsilon < 1$ such that for any solution $x(t) = (S(t), E(t), A(t), I(t))$ with $x(0) \in \Omega$, it satisfies*

$$\min \left\{ \liminf_{t \rightarrow \infty} S(t), \liminf_{t \rightarrow \infty} E(t), \liminf_{t \rightarrow \infty} I(t), \liminf_{t \rightarrow \infty} R(t) \right\} \geq \epsilon. \quad (4.1)$$

Theorem 4.3. *If $R_0 > 1$, then the endemic equilibrium P^* is globally asymptotically stable in the interior of Ω .*

Proof. Using the geometric approach Lemma 3.1 in [28], from Definition 4.2, we know that there exists $\tau > 0$ such that for $t > \tau$, we have

$$\epsilon \leq S(t), E(t), I(t), R(t) \leq 1 - \epsilon. \quad (4.2)$$

The Jacobian matrix of the system (2.1) can be expressed as follows:

$$J = \begin{bmatrix} -\beta I - (\mu + \sigma) & 0 & -\beta S & \delta \\ \beta I & -(\varepsilon + \mu) & \beta S & 0 \\ 0 & \varepsilon & -(\gamma + \mu) & 0 \\ \sigma & 0 & \gamma & -(\delta + \mu) \end{bmatrix}.$$

The third additive compound matrix of the Jacobian matrix has the following form:

$$J^{[3]} = \begin{bmatrix} -3\mu & 0 & 0 & \delta \\ \gamma & -3\mu & \beta S & \beta S \\ 0 & \varepsilon & -3\mu & 0 \\ \sigma & 0 & \beta I & -3\mu \end{bmatrix} + \Psi,$$

where

$$\Psi = \begin{bmatrix} -(\beta I + \sigma + \varepsilon + \gamma) & 0 & 0 & 0 \\ 0 & -(\beta I + \sigma + \varepsilon + \delta) & 0 & 0 \\ 0 & 0 & -(\beta I + \sigma + \gamma + \delta) & 0 \\ 0 & 0 & 0 & -(\varepsilon + \gamma + \delta) \end{bmatrix}.$$

Let $P_f, P(x), \nu$, where c is a positive constant such that $\frac{\gamma+\mu}{\sigma+\gamma+\delta+2\mu} < c < \frac{\beta I + \sigma + \delta + \mu}{\gamma + \beta + \beta \varepsilon}$. Then direct computation shows

$$P_f = \{\dot{R}, c\dot{I}, \dot{E}, \dot{S}\}, P(x) = \text{diag}\{R, cI, E, S\}, \nu = -\mu I_4.$$

By calculating $B(t)$, we obtain the following formula:

$$B(t) = P_f P^{-1} + P J^{[3]} P^{-1} - \nu I_4$$

$$= \begin{bmatrix} -(\beta I + \sigma + \varepsilon + \gamma) & 0 & 0 & \frac{\delta R}{S} \\ \frac{\gamma c I}{R} & -(\beta I + \sigma + \varepsilon + \delta) & \frac{\beta c S I}{E} & \beta c I \\ 0 & \frac{\varepsilon E}{c I} & -(\beta I + \sigma + \gamma + \delta) & 0 \\ \frac{\sigma S}{R} & 0 & \frac{\beta S I}{E} & -(\varepsilon + \gamma + \delta) \end{bmatrix} + \Phi,$$

where

$$\Phi = \begin{bmatrix} \frac{\dot{R}}{R} - 2\mu & 0 & 0 & 0 \\ 0 & \frac{\dot{I}}{I} - 2\mu & 0 & 0 \\ 0 & 0 & \frac{\dot{E}}{E} - 2\mu & 0 \\ 0 & 0 & 0 & \frac{\dot{S}}{S} - 2\mu \end{bmatrix}.$$

Rewrite the equations of the system (2.1) in the following form:

$$\begin{aligned} \frac{\delta R}{S} &= \beta I + (\mu + \sigma) - \frac{b(1-p)}{S} + \frac{S'}{S}, \\ \frac{\beta S I}{E} &= (\varepsilon + \mu) + \frac{E'}{E}, \quad \varepsilon \frac{E}{I} = (\gamma + \mu) + \frac{I'}{I}, \\ \frac{\sigma S}{R} &= (\delta + \mu) - \frac{bp}{R} - \frac{\gamma I}{R} + \frac{R'}{R}. \end{aligned} \tag{4.3}$$

Then, using (4.1) and (4.2), we have

$$\begin{aligned}
h_1(t) &= b_{11}(t) + \sum_{j \neq 1} |b_{1j}(t)| \\
&= -(\beta I + \sigma + \varepsilon + \gamma) - 3\mu + \frac{\delta R}{S} + \frac{R'}{R} + \mu \\
&= -(\beta I + \sigma + \varepsilon + \gamma) - 2\mu + \frac{R'}{R} + \frac{S'}{S} - \frac{b(1-p)}{S} + \beta I + \mu + \sigma \\
&= -(\varepsilon + \gamma + \mu) - \frac{b(1-p)}{S} + \frac{R'}{R} + \frac{S'}{S} \\
&\leq -(\varepsilon + \gamma + \mu) + \frac{R'}{R} + \frac{S'}{S}, \\
h_2(t) &= b_{22}(t) + \sum_{j \neq 1} |b_{2j}(t)| \\
&= \frac{c\gamma I}{R} - (\beta I + \sigma + \varepsilon + \delta) - 3\mu + \frac{c\beta S I}{E} + c\beta I + \frac{I'}{I} + \mu \\
&= \frac{c\gamma I}{R} - (\beta I + \sigma + \varepsilon + \delta) - 2\mu + c\beta I + \frac{I'}{I} + \frac{E'}{E} + \varepsilon + \mu \\
&= \frac{c\gamma I}{R} - (\beta I + \sigma + \delta + \mu) + c\beta I + \frac{I'}{I} + \frac{E'}{E} \\
&= c\left(\frac{\gamma I}{R} + \beta I\right) - (\beta I + \sigma + \delta + \mu) + \frac{I'}{I} + \frac{E'}{E} \\
&\leq c(\gamma + \beta - \beta\varepsilon) - (\beta I + \sigma + \delta + \mu) + \frac{I'}{I} + \frac{E'}{E}, \\
h_3(t) &= b_{33}(t) + \sum_{j \neq 1} |b_{3j}(t)| \\
&= \frac{\varepsilon E}{cI} - (\beta I + \sigma + \gamma + \delta) - 3\mu + \frac{E'}{E} + \mu \\
&= \frac{1}{c}\left(\frac{I'}{I} + \gamma + \mu\right) - (\beta I + \sigma + \gamma + \delta) - 2\mu + \frac{E'}{E} \\
&= \frac{1}{c}(\gamma + \mu) - (\sigma + \gamma + \delta) - 2\mu - \beta I + \frac{I'}{cI} + \frac{E'}{E} \\
&\leq \frac{1}{c}(\gamma + \mu) - (\sigma + \gamma + \delta + 2\mu) + \frac{I'}{cI} + \frac{E'}{E},
\end{aligned}$$

and

$$\begin{aligned}
h_4(t) &= b_{44}(t) + \sum_{j \neq 1} |b_{4j}(t)| \\
&= \frac{\sigma S}{R} + \frac{\beta I S}{E} - (\varepsilon + \gamma + \delta) - 3\mu + \frac{S'}{S} + \mu \\
&= \frac{R'}{R} - \frac{bp}{R} - \frac{\gamma I}{R} + (\delta + \mu) + \frac{E'}{E} + (\varepsilon + \mu) - (\varepsilon + \gamma + \delta + 2\mu) + \frac{S'}{S} \\
&= -\frac{bp}{R} - \frac{\gamma I}{R} - \gamma + \frac{R'}{R} + \frac{E'}{E} + \frac{S'}{S} \\
&\leq -\gamma + \frac{R'}{R} + \frac{E'}{E} + \frac{S'}{S}.
\end{aligned}$$

Set

$$\begin{aligned}\tilde{h}_1(t) &= -(\varepsilon + \gamma + \mu) + \frac{R'}{R} + \frac{S'}{S}, \\ \tilde{h}_2(t) &= c(\gamma + \beta - \beta\epsilon) - (\beta I + \sigma + \delta + \mu) + \frac{I'}{I} + \frac{E'}{E}, \\ \tilde{h}_3(t) &= \frac{1}{c}(\gamma + \mu) - (\sigma + \gamma + \delta + 2\mu) + \frac{I'}{cI} + \frac{E'}{E},\end{aligned}$$

and

$$\tilde{h}_4(t) = -\gamma + \frac{R'}{R} + \frac{E'}{E} + \frac{S'}{S}.$$

Utilize the matrix $C(t)$ from condition (H4) in [28]

$$C(t) = \text{diag} \{ \tilde{h}_1(t), \tilde{h}_2(t), \tilde{h}_3(t), \tilde{h}_4(t) \}.$$

From condition (4.2), we can derive

$$\lim_{t \rightarrow \infty} \frac{1}{t} \int_0^t \tilde{h}_i(\xi) d\xi = \tilde{H}_i < 0,$$

where

$$\tilde{H}_1 = -(\varepsilon + \gamma + \mu), \tilde{H}_2 = c(\gamma + \beta - \beta\epsilon) - (\beta I + \sigma + \delta + \mu),$$

and

$$\tilde{H}_3 = \frac{1}{c}(\gamma + \mu) - (\sigma + \gamma + \delta + 2\mu), \tilde{H}_4 = -\gamma.$$

We can conclude that \tilde{H}_1 and \tilde{H}_4 are strictly less than 0. If c lies within the aforementioned defined interval, then \tilde{H}_2 and \tilde{H}_3 are also strictly less than 0. The above results indicate that matrix $B(t)$ satisfies $\limsup_{t \rightarrow \infty} \frac{1}{t} \int_0^t \mu(B(s)) ds \leq \max_i \tilde{H}_i < 0$. According to Theorem 2.6 in [28], we deduce that the endemic equilibrium point p^* is globally asymptotically stable.

5. Bifurcation analysis

We simplify and change the variables on the system (2.1). Let $S = y_1$, $E = y_2$, $I = y_3$, and $R = y_4$, so that $N = y_1 + y_2 + y_3 + y_4$. By substituting variable $\mathbf{Y} = (y_1, y_2, y_3, y_4)^T$ into the system (2.1), it can be expressed in the following form:

$$\frac{d\mathbf{Y}}{dt} = (g_1, g_2, g_3, g_4)^T,$$

where

$$\begin{cases} y'_1(t) = g_1 := b(1-p) - \beta y_1 y_3 - (\mu + \sigma) y_1 + \delta y_4, \\ y'_2(t) = g_2 := \beta y_1 y_3 - (\varepsilon + \mu) y_2, \\ y'_3(t) = g_3 := \varepsilon y_2 - (\gamma + \mu) y_3, \\ y'_4(t) = g_4 := bp + \gamma y_3 - (\delta + \mu) y_4 + \sigma y_1. \end{cases} \quad (5.1)$$

We assume that β is the bifurcation parameter and $\delta + \mu > \mu p$. When $R_0 = 1$, we can obtain

$$\beta = \beta^* = \frac{\mu(\mu + \delta + \sigma)}{b(\delta + \mu - \mu p)} \cdot \frac{(\varepsilon + \mu)(\gamma + \mu)}{\varepsilon}. \quad (5.2)$$

The Jacobian matrix eigenvalues for the system (2.1), evaluated at P_0 with $\beta = \beta^*$, are presented as

$$\lambda_1 = 0, \lambda_2 = -\mu, \lambda_3 = -(\gamma + \mu), \text{ and } \lambda_4 = -(\mu + \sigma + \delta).$$

Thus, $\lambda_1 = 0$ is a simple zero eigenvalue, and the other eigenvalues have negative real parts. Therefore, when $\beta = \beta^*$, the first assumption of Theorem 4.1 in [29] is satisfied. Hence, a nonnegative right eigenvector corresponding to the zero eigenvalue λ_1 is given by

$$\mathbf{v} = (v_1, v_2, v_3, v_4)^T = \begin{bmatrix} -(\varepsilon\gamma + (\delta + \mu)(\varepsilon + \gamma + \mu)) \\ (\gamma + \mu)(\delta + \mu + \sigma) \\ \varepsilon(\delta + \mu + \sigma) \\ \varepsilon\gamma - \sigma(\varepsilon + \gamma + \mu) \end{bmatrix}. \quad (5.3)$$

Furthermore, we find the left eigenvector w related to the eigenvalue $\lambda_1 = 0$, satisfies $w \cdot v = 1$, where

$$\mathbf{w} = (w_1, w_2, w_3, w_4)^T = \begin{bmatrix} 0 \\ \frac{1}{(\delta + \mu + \sigma)(\gamma + \varepsilon + 2\mu)} \\ \frac{\varepsilon + \mu}{\varepsilon(\delta + \mu + \sigma)(\gamma + \varepsilon + 2\mu)} \\ 0 \end{bmatrix}. \quad (5.4)$$

The coefficients \hat{a} and \hat{b} , as defined by Theorem 4.1 in [29], are determined through the following calculations. For the system of Eqs (5.1), the corresponding non-zero second partial derivatives of the functions g_i , evaluated at (P_0, β^*) , can be expressed as follows:

$$\begin{aligned} \frac{\partial^2 g_1}{\partial y_1 \partial y_3}(P_0, \beta^*) &= \frac{\partial^2 g_1}{\partial y_3 \partial y_1}(P_0, \beta^*) = -\beta^*, \\ \frac{\partial^2 g_2}{\partial y_1 \partial y_3}(P_0, \beta^*) &= \frac{\partial^2 g_2}{\partial y_3 \partial y_1}(P_0, \beta^*) = \beta^*, \\ \frac{\partial^2 g_1}{\partial y_3 \partial \beta}(P_0, \beta^*) &= -\frac{b(\delta + \mu - \mu p)}{\mu(\mu + \delta + \sigma)}, \end{aligned}$$

and

$$\frac{\partial^2 g_2}{\partial y_3 \partial \beta}(P_0, \beta^*) = \frac{b(\delta + \mu - \mu p)}{\mu(\mu + \delta + \sigma)}. \quad (5.5)$$

Then, using the expressions (5.2)–(5.5), we calculate that \hat{a} and \hat{b}

$$\hat{a} = \sum_{k,i,j=1}^4 v_k w_i w_j \frac{\partial^2 g_k}{\partial y_i \partial y_j}(P_0, \beta^*) = 0,$$

and

$$\hat{b} = \sum_{k,i=1}^4 v_k w_i \frac{\partial^2 g_k}{\partial y_i \partial \beta}(P_0, \beta^*) = \frac{(\varepsilon + \mu)}{\beta^*(\gamma + \varepsilon + 2\mu)}.$$

It is found that the coefficient \hat{b} is always positive. Combining the actual parameters and Theorem 4.1 in [29], it can be obtained that the system behaves as a standard forward bifurcation at $R_0 = 1$, rather than a backward bifurcation. Therefore, we have the following theorem.

Theorem 5.1. Assume that $R_0 = 1$, then the system (2.1) has a forward bifurcation.

We set the parameters as $\mu = 1/70$, $N = 1000$, $p = 0.8$, $\sigma = 0.3$, $\delta = 0.1$, $\varepsilon = 365/10$, and $\gamma = 365/14$. The x-axis represents the value of the basic reproduction number R_0 , ranging from 0 to 5, and β varies proportionally with R_0 . The y-axis represents the number of infected individuals at the equilibrium point. A forward bifurcation diagram is drawn as shown in Figure 2.

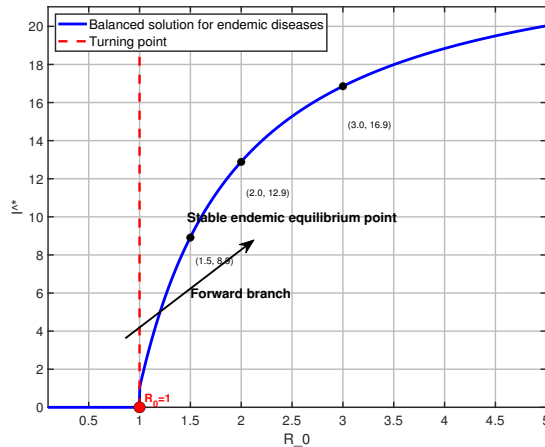


Figure 2. Forward bifurcation diagram of model (2.1).

6. A special case

In this section, we consider a special case where recovered individuals no longer lose immunity and become susceptible individuals. Let $\delta = 0$, and the system (2.1) becomes the following system:

$$\begin{cases} \frac{dS}{dt} = b(1-p) - \beta SI - (\mu + \sigma)S, \\ \frac{dE}{dt} = \beta SI - (\varepsilon + \mu)E, \\ \frac{dI}{dt} = \varepsilon E - (\gamma + \mu)I, \\ \frac{dR}{dt} = bp + \gamma I - \mu R + \sigma S. \end{cases} \quad (6.1)$$

The initial triad of equations in the system (6.1) exhibits structural independence from variable R . We consider the dynamics of the subsystem

$$\begin{cases} \frac{dS}{dt} = b(1-p) - \beta SI - (\mu + \sigma)S, \\ \frac{dE}{dt} = \beta SI - (\varepsilon + \mu)E, \\ \frac{dI}{dt} = \varepsilon E - (\gamma + \mu)I. \end{cases} \quad (6.2)$$

The basic reproduction number of this system is the same as (3.2) when $\delta = 0$; therefore

$$R'_0 = \frac{\beta\varepsilon}{(\varepsilon + \mu)(\gamma + \mu)} \cdot \frac{b(1 - p)}{(\mu + \sigma)}.$$

Theorem 6.1. *If $R'_0 > 1$, then the endemic equilibrium point $P_1^* = (S_1^*, E_1^*, I_1^*)$ of the system (6.2) is globally asymptotically stable inside Ω .*

Proof. For the endemic equilibrium point $P_1^* = (S_1^*, E_1^*, I_1^*)$, it must satisfy the following system of equations:

$$\begin{aligned} b(1 - p) - \beta S_1^* I_1^* - (\mu + \sigma) S_1^* &= 0, \\ \beta S_1^* I_1^* - (\varepsilon + \mu) E_1^* &= 0, \end{aligned} \quad (6.3)$$

and

$$\varepsilon E_1^* - (\gamma + \mu) I_1^* = 0.$$

Define the following Lyapunov function:

$$V = B_1(S - S_1^* - S_1^* \ln S) + B_2(E - E_1^* - E_1^* \ln E) + B_3(I - I_1^* - I_1^* \ln I), \quad (6.4)$$

where B_1, B_2, B_3 are non-negative constants. Using (6.3), the derivative of V along the solution of (6.2), we have

$$\begin{aligned} \dot{V} &= B_1 \left(1 - \frac{S_1^*}{S}\right) \dot{S} + B_2 \left(1 - \frac{E_1^*}{E}\right) \dot{E} + B_3 \left(1 - \frac{I_1^*}{I}\right) \dot{I} \\ &= B_1 \left(1 - \frac{S_1^*}{S}\right) \beta S_1^* I_1^* \left(1 - \frac{SI}{S_1^* I_1^*}\right) + B_1 \left(1 - \frac{S_1^*}{S}\right) S_1^* (\mu + \sigma) \left(1 - \frac{S}{S_1^*}\right) \\ &\quad + B_2 \left(1 - \frac{E_1^*}{E}\right) \left[\beta S_1^* I_1^* \left(\frac{SI}{S_1^* I_1^*} - \frac{E}{E_1^*} \right) \right] \\ &\quad + B_3 \left(1 - \frac{I_1^*}{I}\right) \left[\varepsilon E_1^* \left(\frac{E}{E_1^*} - \frac{I}{I_1^*} \right) \right]. \end{aligned}$$

Let, $x = \frac{S}{S_1^*}$, $y = \frac{E}{E_1^*}$, $z = \frac{I}{I_1^*}$, then

$$\begin{aligned} \dot{V} &= B_1 \beta S_1^* I_1^* \left(1 - \frac{1}{x}\right) (1 - xz) + B_1 \left(1 - \frac{1}{x}\right) S_1^* (\mu + \sigma) (1 - x) \\ &\quad + B_2 \left(1 - \frac{1}{y}\right) [\beta S_1^* I_1^* (xz - y)] + B_3 \left(1 - \frac{1}{z}\right) [\varepsilon E_1^* (y - z)] \\ &= B_1 S_1^* (\mu + \sigma) \frac{(1 - x)^2}{x} + (B_1 \beta S_1^* I_1^* + B_2 \beta S_1^* I_1^* + B_3 \varepsilon E_1^*) \\ &\quad + xz (B_2 \beta S_1^* I_1^* - B_1 \beta S_1^* I_1^*) + y (B_3 \varepsilon E_1^* - B_2 \beta S_1^* I_1^*) \\ &\quad + z (B_1 \beta S_1^* I_1^* - B_3 \varepsilon E_1^*) - \frac{1}{x} B_1 \beta S_1^* I_1^* - \frac{xz}{y} B_2 \beta S_1^* I_1^* - \frac{y}{z} B_3 \varepsilon E_1^*. \end{aligned}$$

Variables x, y, z are non-negative, to ensure the Lyapunov function remains negative definite. Setting the terms involving x, y, z to zero, we obtain

$$B_2 \beta S_1^* I_1^* - B_1 \beta S_1^* I_1^* = 0,$$

$$B_3\varepsilon E_1^* - B_2\beta S_1^* I_1^* = 0,$$

and

$$B_1\beta S_1^* I_1^* - B_3\varepsilon E_1^* = 0.$$

By the above system of equations, the solution to the problem is obtained

$$B_1 = B_2 = 1, B_3 = \frac{\beta S_1^* I_1^*}{\varepsilon E_1^*},$$

therefore

$$\begin{aligned} \dot{V} &= -S_1^* (\mu + \sigma) \frac{(1-x)^2}{x} + 3\beta S_1^* I_1^* - \frac{1}{x} \beta S_1^* I_1^* - \frac{xz}{y} \beta S_1^* I_1^* - \frac{y}{z} \varepsilon E_1^* \\ &= -S_1^* (\mu + \sigma) \frac{(1-x)^2}{x} + \left(3 - \frac{1}{x} - \frac{xz}{y} - \frac{y}{z}\right) \beta S_1^* I_1^*. \end{aligned}$$

Due to the fact that the average value of the calculated numbers is greater than or equal to the average value of several values, then $3 - \frac{1}{x} - \frac{xz}{y} - \frac{y}{z} \leq 0$ if and only if $x, y, z > 0$, and $3 - \frac{1}{x} - \frac{xz}{y} - \frac{y}{z} = 0$ if and only if $x = y = z = 1$. Therefore, for the system (6.2) in the set $\{(x, y, z) : \dot{V} = 0\}$, the maximum invariant set is the singleton $(1, 1, 1)$. By the LaSalle invariance principle, the local equilibrium point of the system (6.2) is globally asymptotically stable.

7. Numerical simulation

In this section, we conduct numerical simulations on the disease transmission process of the SEIR model and explain the analysis results obtained.

Table 1. Numerical values of parameters.

Parameter	Description	Value	Unit
N	Total population	67,081,234	people
b	Daily births	1,820	people/day
ε	Progression rate of exposed compartment to infective compartment	0.2	per day
μ	Natural mortality rate	2.49×10^{-5}	per day
γ	Recovery rate	0.0714	per day
β	Infection rate	1.0×10^{-8}	per day-person
σ	Vaccination rate of susceptibles	Variable	per day
p	Vaccination proportion at birth	0.85	dimensionless
δ	Immunity waning rate	0.00417	per day

We chose the UK as the simulation country because it has relatively complete data records on COVID-19 and vaccination statistics. We used the population data of the UK in 2020 and assumed that a portion of the population had been vaccinated at the beginning of the simulation. The parameter values will be set based on the actual data of the UK. Through numerical solutions, we obtain the dynamic process of changes in the population quantities of each group in the model over time. In particular, $R_0 = 0.986 < 1$ is calculated, indicating that the transmissibility of the disease is relatively low and cannot trigger large-scale epidemics.

The numerical outcomes in Figure 3 indicate that the susceptible $S(t)$ curve rapidly decreases at the initial stage, then gradually rises and eventually tends to be stable over time. This indicates that in the early stages of the disease, most susceptibles are infected due to contact with infected individuals, leading to a rapid decrease in the number of susceptibles. The exposed $E(t)$ initially rises rapidly and then shows a downward trend. This indicates that although individuals in the incubation period do not show symptoms, the exposed will eventually become infected, leading to a decrease in the population of exposed individuals. The number of infected individuals $I(t)$ grows rapidly at the initial stage, then gradually slows down, and finally tends to be stable. This reflects that after the incubation period, infected individuals quickly enter the infected state, and with the passage of time, they are gradually cured or die, consequently inducing asymptotic convergence of infection prevalence toward epidemiologic steady state. The results in Figure 4 indicate that the recovered $R(t)$ curve gradually increases and eventually stabilizes. This indicates that with the passage of time, more and more infected individuals enter the recovered group through recovery or treatment, thereby increasing the number of recovered individuals and eventually reaching a stable state. This visualizes Theorem 4.1, which states that when $R_0 < 1$, the system approaches a disease-free state.

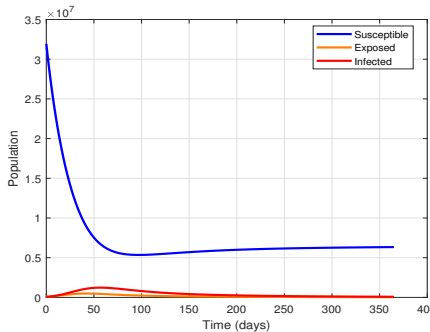


Figure 3. The time variation graphs of $S(t)$, $E(t)$, and $I(t)$ when $R_0 < 1$.

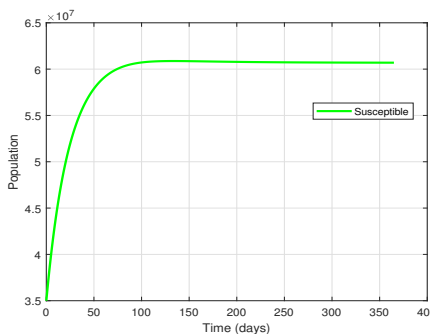


Figure 4. The time variation graphs of $R(t)$ when $R_0 < 1$.

Keep all other parameters unchanged and change the size of R_0 by adjusting the value of $\sigma = 0.05$. Calculate the basic reproduction number $R_0 = 6.88 > 1$, indicating that the disease has strong transmission ability. As shown in Figure 5, under the condition $R_0 > 1$, the number of susceptible $S(t)$ rapidly decreases at the initial stage and then tends to be stable, reflecting that most susceptibles are infected. The exposed $E(t)$ and infected $I(t)$ increase slowly at the initial stage, then decrease,

and eventually tend to 0. As shown in Figure 6, the dynamic evolution of recovered individuals $R(t)$, exhibit monotonic growth followed by asymptotic stabilization. This illustrates Theorem 4.3, which states that when $R_0 > 1$, the disease persists in the population.

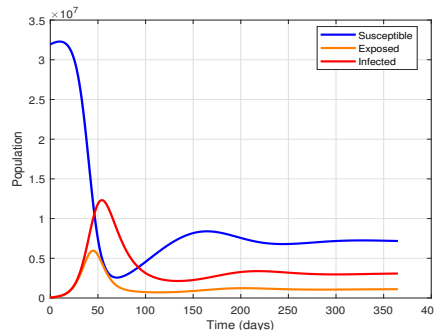


Figure 5. The time variation graphs of $S(t)$, $E(t)$, and $I(t)$ when $R_0 > 1$.

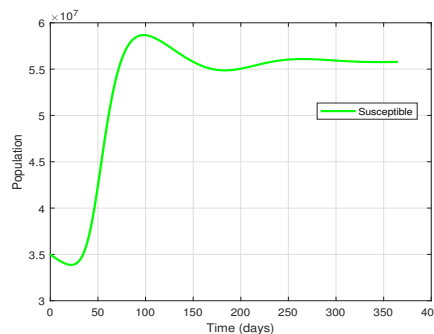


Figure 6. The time variation graphs of $R(t)$ when $R_0 > 1$.

8. Sensitivity analysis

This section performs sensitivity analysis on the basic reproduction number R_0 to quantify how the system parameters influence epidemic transmission dynamics, so that we can control specific parameters to seek effective disease control measures. As shown in Tables 2 and 3, parameters greater than zero will positively affect the change in R_0 , being directly proportional to R_0 . Conversely, if the sensitivity index is negative, it is inversely proportional to R_0 .

Table 2. Sensitivity index when $R_0 < 1$.

Parameter	Sensitivity index	Parameter	Sensitivity index
b	1.000	ε	0.00012464
μ	-1.0002	γ	-0.99965
β	1.000	δ	0.90263
σ	-0.90295		

Table 3. Sensitivity index when $R_0 > 1$.

Parameter	Sensitivity index	Parameter	Sensitivity index
b	1.000	ε	0.00012464
μ	-1.0036	γ	-0.99965
β	1.000	δ	0.32615
σ	-0.32302		

Definition 8.1. The normalized forward sensitivity index of R_0 , the corresponding parameter is defined in [30] as

$$\Upsilon_{\varepsilon}^{R_0} = \frac{\partial R_0}{\partial \varepsilon} \cdot \frac{\varepsilon}{R_0}.$$

The basic reproduction number R_0 exhibits a strong positive correlation with the natural birth rate b , as shown in Figure 7(a). This relationship arises because a higher birth rate introduces a larger proportion of unvaccinated susceptible individuals ($1 - p$) into the population, thereby expanding the pool of potential hosts for disease transmission. Figure 7(b) demonstrates that R_0 increases monotonically with the immunity loss rate β . A higher β accelerates the reversion of individuals to the infection compartment, effectively replenishing the susceptible population over time. As illustrated in Figure 7(c), R_0 decreases as the natural death rate μ increases. Elevated mortality reduces the average duration of susceptibility and infectiousness, thereby limiting opportunities for transmission. Figure 7(d) reveals that R_0 increases slowly with the increase of immunity waning rate δ .

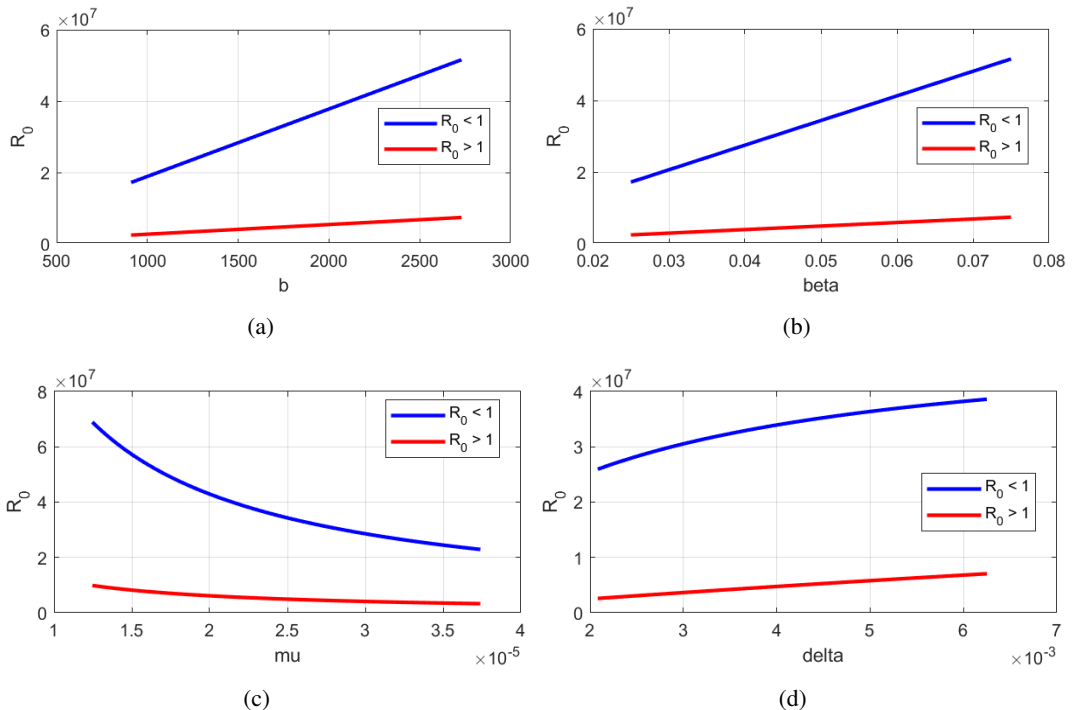


Figure 7. (a) The link between R_0 and b ; (b) The link between R_0 and β ; (c) The link between R_0 and μ ; (d) The link between R_0 and σ .

All relationships exhibit monotonicity within the tested parameter ranges, indicating model stability and predictable control outcomes. Critically, these figures emphasize the need for synergistic interventions: For instance, regions with high natural birth rate require proportionally higher vaccination rate to offset demographic pressures. Public health strategies should prioritize scalable vaccination infrastructure and adaptive booster schedules to address immunity waning (δ), while demographic policies may complement disease control efforts in high-fertility populations.

Use of AI tools declaration

The authors declare they have not used Artificial Intelligence (AI) tools in the creation of this article.

Acknowledgments

This research was supported by the National Natural Science Foundation of China (12426515), the Jiangsu Provincial Higher Education Natural Science Research (24KJD110006), the Natural Science Foundation of the Jiangsu Higher Education Institutions of China (23KJB110024) and the Xuzhou Youth Science and Technology Talent Project (KC23032).

Conflict of interest

The authors declare there are no conflicts of interest.

References

1. J. Yu, D. Jiang, N. Shi, Global stability of two-group SIR model with random perturbation, *J. Math. Anal. Appl.*, **360** (2009), 235–244. <https://doi.org/10.1016/j.jmaa.2009.06.050>
2. J. Liu, Y. Zhou, Global stability of an SIRS epidemic model with transport-related infection, *Chaos, Solitons Fractals*, **40** (2009), 145–158. <https://doi.org/10.1016/j.chaos.2007.07.047>
3. D. Knipl, S. M. Moghadas, The potential impact of vaccination on the dynamics of dengue infections, *Bull. Math. Biol.*, **77** (2015), 2212–2230. <https://doi.org/10.1007/s11538-015-0120-6>
4. T. M. Chen, J. Rui, Q. P. Wang, Z. Y. Zhao, J. A. Cui, L. Yin, A mathematical model for simulating the phase-based transmissibility of a novel coronavirus, *Infect. Dis. Poverty*, **9** (2020), 1–8. <https://doi.org/10.1186/s40249-020-00640-3>
5. S. Han, C. Lei, Global stability of equilibria of a diffusive SEIR epidemic model with nonlinear incidence, *Appl. Math. Lett.*, **98** (2019), 114–120. <https://doi.org/10.1016/j.aml.2019.05.045>
6. S. Zhi, D. Bai, Y. Su, Turing patterns induced by cross-diffusion in a predator-prey model with Smith-type prey growth and additive predation effects, *Chaos, Solitons Fractals*, **202** (2026), 117522. <https://doi.org/10.1016/j.chaos.2025.117522>
7. W. O. Kermack, A. G. McKendrick, A contribution to the mathematical theory of epidemics, *Proc. R. Soc. A*, **115** (1927), 700–721. <https://doi.org/10.1098/rspa.1927.0118>
8. W. Ma, M. Song, Y. Takeuchi, Global stability of an SIR epidemic model with time delay, *Appl. Math. Lett.*, **17** (2004), 1141–1145. <https://doi.org/10.1016/j.aml.2003.11.005>

9. Y. Yang, J. Zhou, C. H. Hsu, Threshold dynamics of a diffusive SIRI model with nonlinear incidence rate, *J. Math. Anal. Appl.*, **478** (2019), 874–896. <https://doi.org/10.1016/j.jmaa.2019.05.059>

10. S. Zhi, H. Niu, Y. Su, X. L. Han, Influence of human behavior on COVID-19 dynamics based on a reaction-diffusion model, *Qual. Theory Dyn. Syst.*, **22** (2023), 113. <https://doi.org/10.1007/s12346-023-00810-2>

11. S. Annas, M. I. Pratama, M. Rifandi, W. Sanusi, S. Side, Stability analysis and numerical simulation of SEIR model for pandemic COVID-19 spread in Indonesia, *Chaos, Solitons Fractals*, **139** (2020), 110072. <https://doi.org/10.1016/j.chaos.2020.110072>

12. M. J. Keeling, P. Rohani, *Modeling Infectious Diseases in Humans and Animals*, Princeton University Press, 2008. <https://doi.org/10.1515/9781400841035>

13. Q. Yang, D. Jiang, N. Shi, C. Ji, The ergodicity and extinction of stochastically perturbed SIR and SEIR epidemic models with saturated incidence, *J. Math. Anal. Appl.*, **388** (2012), 248–271. <https://doi.org/10.1016/j.jmaa.2011.11.072>

14. R. K. Upadhyay, A. K. Pal, S. Kumari, P. Roy, Dynamics of an SEIR epidemic model with nonlinear incidence and treatment rates, *Nonlinear Dyn.*, **96** (2019), 2351–2368. <https://doi.org/10.1007/s11071-019-04926-6>

15. A. Khan, G. Zaman, Global analysis of an age-structured SEIR endemic model, *Chaos, Solitons Fractals*, **108** (2018), 154–165. <https://doi.org/10.1016/j.chaos.2018.01.037>

16. J. Jiao, Z. Liu, S. Cai, Dynamics of an SEIR model with infectivity in incubation period and homestead-isolation on the susceptible, *Appl. Math. Lett.*, **107** (2020), 106442. <https://doi.org/10.1016/j.aml.2020.106442>

17. J. Li, Y. Yang, Y. Zhou, Global stability of an epidemic model with latent stage and vaccination, *Appl. Math. Lett.*, **12** (2011), 2163–2173. <https://doi.org/10.1016/j.nonrwa.2010.12.030>

18. S. Zhi, Y. Su, H. Niu, J. Cao, Analysis of a diffusive vector-borne disease model with nonlinear incidence and nonlocal delayed transmission, *Z. Angew. Math. Phys.*, **75** (2024), 227. <https://doi.org/10.1007/s00033-024-02377-7>

19. S. Zhi, Y. Su, H. Niu, L. Qiang, The threshold dynamics of a waterborne pathogen model with seasonality in a polluted environment, *Acta Math. Sci.*, **44** (2024), 2165–2189. <https://doi.org/10.1007/s10473-024-0607-z>

20. S. Zhi, H. Niu, Y. Su, Global dynamics of a diffusive SIRS epidemic model in a spatially heterogeneous environment, *Appl. Anal.*, **104** (2025), 390–418. <https://doi.org/10.1080/00036811.2024.2367667>

21. C. Sun, Y. Lin, S. Tang, Global stability for an special SEIR epidemic model with nonlinear incidence rates, *Chaos, Solitons Fractals*, **33** (2007), 290–297. <https://doi.org/10.1016/j.chaos.2005.12.028>

22. A. D’Onofrio, Stability properties of pulse vaccination strategy in SEIR epidemic model, *Math. Biosci.*, **179** (2002), 57–72. [https://doi.org/10.1016/S0025-5564\(02\)00095-0](https://doi.org/10.1016/S0025-5564(02)00095-0)

23. G. Li, Z. Jin, Global stability of a SEIR epidemic model with infectious force in latent, infected and immune period, *Chaos, Solitons Fractals*, **25** (2005), 1177–1184. <https://doi.org/10.1016/j.chaos.2004.11.062>

24. C. Sun, Y. H. Hsieh, Global analysis of an SEIR model with varying population size and vaccination, *Appl. Math. Modell.*, **34** (2010), 2685–2697. <https://doi.org/10.1016/j.apm.2009.12.005>

25. Q. Wen, H. Li, Y. Su, Long-time dynamics of an infection age-structure SIR epidemic model with nonlocal diffusion of Neumann type, *J. Math. Anal. Appl.*, **554** (2026), 129987. <https://doi.org/10.1016/j.jmaa.2025.129987>

26. P. Van den Driessche, J. Watmough, Reproduction numbers and sub-threshold endemic equilibria for compartmental models of disease transmission, *Math. Biosci.*, **180** (2002), 29–48. [https://doi.org/10.1016/S0025-5564\(02\)00108-6](https://doi.org/10.1016/S0025-5564(02)00108-6)

27. J. P. La Salle, *The Stability of Dynamical Systems*, SIAM, 1976.

28. G. Lu, Z. Lu, Geometric approach to global asymptotic stability for the SEIRS models in epidemiology, *Nonlinear Anal. Real World Appl.*, **36** (2017), 20–43. <https://doi.org/10.1016/j.nonrwa.2016.12.005>

29. C. Castillo-Chavez, B. Song, Dynamical models of tuberculosis and their applications, *Math. Biosci. Eng.*, **1** (2004), 361–404. <https://doi.org/10.3934/mbe.2004.1.361>

30. N. Chitnis, J. M. Hyman, J. M. Cushing, Determining important parameters in the spread of malaria through the sensitivity analysis of a mathematical model, *Bull. Math. Biol.*, **70** (2008), 1272–1296. <https://doi.org/10.1007/s11538-008-9299-0>



AIMS Press

© 2025 the Author(s), licensee AIMS Press. This is an open access article distributed under the terms of the Creative Commons Attribution License (<https://creativecommons.org/licenses/by/4.0>)